

Antideuterons from Dark Matter Decay

Alejandro Ibarra and David Tran*

*Physik-Department T30d, Technische Universität München,
James-Franck-Straße, 85748 Garching, Germany.*

Abstract

Recent observations of a large excess of cosmic-ray positrons at high energies have raised a lot of interest in leptonic decay modes of dark matter particles. Nevertheless, dark matter particles in the Milky Way halo could also decay hadronically, producing not only a flux of antiprotons but also a flux of antideuterons. We show that for certain choices of parameters the antideuteron flux from dark matter decay can be much larger than the purely secondary flux from spallation of cosmic rays on the interstellar medium, while the total antiproton flux remains consistent with present observations. We show that if the dark matter particle is sufficiently light, the antideuteron flux from dark matter decay could even be within the reach of planned experiments such as AMS-02 or GAPS. Furthermore, we discuss the prospects to observe the antideuteron flux in the near future if the steep rise in the positron fraction reported by the PAMELA collaboration is interpreted in terms of the decay of dark matter particles.

April 2009

*E-mail addresses: alejandro.ibarra@ph.tum.de, david.tran@ph.tum.de

1 Introduction

There is mounting evidence for the existence of a hitherto undiscovered elementary particle in the Universe, the dark matter particle, with an abundance which is approximately six times bigger than the abundance of baryons. Dark matter particles are also known to exist in galactic halos through their gravitational influence on the motion of stars [1]. However, although dark matter particles are ubiquitous in the Universe at large, as well as in our own Galaxy, very little is known about their nature and properties.

One of the key questions about the dark matter properties is whether the dark matter particles are stable or not. Indeed, astrophysical and cosmological observations do not require the dark matter particles to be absolutely stable, but only to have a lifetime larger than the age of the Universe. Furthermore, recent evidence for the existence of a primary component in the high energy electron and positron fluxes [2] could be naturally accounted for by the decay of dark matter particles with a mass $m_{\text{DM}} \gtrsim 300$ GeV, which decay preferentially into charged leptons of the first and second generations with a lifetime $\tau_{\text{DM}} \sim 10^{26}$ s [3].

The properties of the dark matter particles are further constrained from observations of the diffuse gamma-ray flux by EGRET [4], as well as from observations of the antiproton flux by PAMELA [5], BESS95 [6], BESS95/97 [7], CAPRICE94 [8], CAPRICE98 [9] and IMAX [10]. More concretely, the good agreement of the theoretical predictions for a purely secondary antiproton flux with the measurements indicates that the contribution to the total antiproton flux from dark matter matter can only be subdominant. On the other hand, the gamma-ray excess in the extragalactic background, revealed by the analysis in [11] after subtracting the galactic foreground, hints at a possible exotic component of diffuse gamma rays, which will be confirmed or refuted by Fermi in the near future.

In this paper we will estimate the antideuteron flux from dark matter decay as a complementary way to determine the properties of the dark matter particle. As pointed out in [12,13], for energies smaller than ~ 3 GeV the expectations for a purely secondary antideuteron flux, due to spallation of cosmic rays on the interstellar medium, lie below the present BESS limit on the antideuteron flux [14], as well as the projected limits for AMS-02 [15,16] and GAPS [17,18]. Therefore, no detection of antideuterons is to

Halo model	α	β	γ	r_c (kpc)
Navarro, Frenk, White [20]	1	3	1	20
Isothermal	2	2	0	3.5
Moore [21]	1.5	3	1.5	28

Table 1: Parameters characterizing some commonly used halo models.

be expected in these experiments if the antideuteron flux is of purely secondary origin. At the same time, a discovery of cosmic antideuterons in the upcoming generation of experiments would be strong evidence for a primary component and, if interpreted as the result of dark matter decay, as evidence for hadronic decays of dark matter particles, which may not be inferred from the antiproton flux due to the large astrophysical background in this channel.

In Section 2 we will review antideuteron production from dark matter decay using the coalescence model. In Section 3 we will review the propagation of antideuterons in the diffusive halo of the Milky Way. In Section 4 we will show our results, and in Section 5 we will finally present our conclusions.

2 Antideuteron Production

We will assume that the Milky Way dark matter halo is populated by dark matter particles with mass m_{DM} , with their distribution following a density profile $\rho(\vec{r})$, where \vec{r} denotes position with respect to the center of the Galaxy. The dark matter distribution is usually parametrized as a spherically symmetric profile

$$\rho(r) = \frac{\rho_0}{(r/r_c)^\gamma [1 + (r/r_c)^\alpha]^{(\beta-\gamma)/\alpha}}, \quad (1)$$

where $r = |\vec{r}|$ and the parameters α , β , γ and r_c are listed in Table 1 for some commonly used halo models. Finally, ρ_0 is a parameter that is adjusted to yield a local halo density of $\rho(r_\odot) = 0.30 \text{ GeV/cm}^3$ [19], with $r_\odot = 8.5 \text{ kpc}$ being the distance of the Sun to the Galactic center.

Dark matter particles at \vec{r} eventually decay with lifetime τ_{DM} , producing antideuterons at a rate per unit energy and unit volume given by

$$Q_{\bar{d}}(E_{\bar{d}}, \vec{r}) = \frac{\rho(\vec{r})}{m_{\text{DM}}\tau_{\text{DM}}} \frac{dN_{\bar{d}}}{dE_{\bar{d}}}, \quad (2)$$

where $dN_{\bar{d}}/dE_{\bar{d}}$ is the energy spectrum of antideuterons produced in the decay.

The production of antideuterons in the fragmentation of weak gauge bosons or Higgs bosons can be described by the coalescence model which assumes that the probability in momentum space of producing an antideuteron is proportional to the product of the probabilities of producing a single antiproton and a single antineutron:

$$\left[\gamma_{\bar{d}} \frac{d^3 N_{\bar{d}}}{d^3 \vec{k}_{\bar{d}}} \right] = \int d^3 \vec{k}_{\bar{p}} d^3 \vec{k}_{\bar{n}} C(\vec{k}_{\bar{p}}, \vec{k}_{\bar{n}}) \left[\gamma_{\bar{p}} \frac{d^3 N_{\bar{p}}}{d^3 \vec{k}_{\bar{p}}}(\vec{k}_{\bar{p}}) \right] \left[\gamma_{\bar{n}} \frac{d^3 N_{\bar{n}}}{d^3 \vec{k}_{\bar{n}}}(\vec{k}_{\bar{n}}) \right] \delta^{(3)}(\vec{k}_{\bar{p}} + \vec{k}_{\bar{n}} - \vec{k}_{\bar{d}}), \quad (3)$$

where γ is a Lorentz factor and $C(\vec{k}_{\bar{p}}, \vec{k}_{\bar{n}})$ is the coalescence function which can only depend on the relative momentum between antiproton and antineutron, $\vec{\Delta} = \vec{k}_{\bar{p}} - \vec{k}_{\bar{n}}$. Using that $\vec{k}_{\bar{d}} = \vec{k}_{\bar{p}} + \vec{k}_{\bar{n}}$, one obtains

$$\left[\gamma_{\bar{d}} \frac{d^3 N_{\bar{d}}}{d^3 \vec{k}_{\bar{d}}} \right] = \int d^3 \vec{\Delta} C(|\vec{\Delta}|) \left[\gamma_{\bar{p}} \frac{d^3 N_{\bar{p}}}{d^3 \vec{k}_{\bar{p}}} \left(\vec{k}_{\bar{p}} = \frac{\vec{k}_{\bar{d}} + \vec{\Delta}}{2} \right) \right] \left[\gamma_{\bar{n}} \frac{d^3 N_{\bar{n}}}{d^3 \vec{k}_{\bar{n}}} \left(\vec{k}_{\bar{n}} = \frac{\vec{k}_{\bar{d}} - \vec{\Delta}}{2} \right) \right]. \quad (4)$$

The coalescence function is strongly peaked at $|\vec{\Delta}| \simeq 0$ since the binding energy of the antideuteron, $B \simeq 2.2$ MeV, is much smaller than its rest mass, $m_{\bar{d}} \simeq 1.88$ GeV. Therefore, the previous expression can be approximated by

$$\left[\gamma_{\bar{d}} \frac{d^3 N_{\bar{d}}}{d^3 \vec{k}_{\bar{d}}} \right] \simeq \int d^3 \vec{\Delta} C(|\vec{\Delta}|) \left[\gamma_{\bar{p}} \frac{d^3 N_{\bar{p}}}{d^3 \vec{k}_{\bar{p}}} \left(\vec{k}_{\bar{p}} = \frac{\vec{k}_{\bar{d}}}{2} \right) \right] \left[\gamma_{\bar{n}} \frac{d^3 N_{\bar{n}}}{d^3 \vec{k}_{\bar{n}}} \left(\vec{k}_{\bar{n}} = \frac{\vec{k}_{\bar{d}}}{2} \right) \right]. \quad (5)$$

It is useful to define the coalescence momentum, p_0 , as

$$\int d^3 \vec{\Delta} C(|\vec{\Delta}|) \equiv \frac{4\pi}{3} p_0^3, \quad (6)$$

which can be interpreted as the maximum relative momentum between the antiproton and the antineutron for which an antideuteron will form by fusion of the two nucleons. The coalescence momentum can be determined experimentally from proton–nucleus collisions, yielding $p_0 \simeq 79$ MeV¹ [22], or from e^+e^- collisions at the Z^0 resonance, yielding $p_0 \simeq 71.8 \pm 3.6$ MeV [23]. Since the decay of weak gauge bosons is precisely the source of antideuterons in the decaying dark matter scenario, we will adopt the latter value $p_0 \simeq 71.8 \pm 3.6$ MeV in the remainder of the paper. Note that the measured coalescence momentum is not far from the estimate obtained by using the antideuteron

¹The uncertainty in the measurement of the hadronic production cross sections translates into a range for the coalescence momentum that was estimated to be $p_0 = 79_{-13}^{+26}$ MeV [13].

binding energy, namely $\sqrt{m_{\bar{p}}B} \sim 46$ MeV, supporting the above physical interpretation of the coalescence momentum.

The dark matter decay produces antideuterons, antiprotons and antineutrons with an isotropic distribution, and consequently

$$\left[\gamma \frac{d^3 N}{d^3 k} \right] = \frac{1}{4\pi m k} \frac{dN}{dE} . \quad (7)$$

Therefore, Eq. (5) can be cast as:

$$\frac{dN_{\bar{d}}}{dE_{\bar{d}}} \simeq \frac{4p_0^3}{3k_{\bar{d}} m_{\bar{p}} m_{\bar{n}}} \left[\frac{dN_{\bar{p}}}{dE_{\bar{p}}} \left(E_{\bar{p}} = \frac{E_{\bar{d}}}{2} \right) \right]^2 , \quad (8)$$

where we have assumed, employing isospin invariance, that the probability of producing an antiproton with momentum $\vec{k}_{\bar{p}}$ in the fragmentation is the same as the probability of producing an antineutron.

3 Propagation

Antideuteron propagation in the Milky Way can be described by a stationary two-zone diffusion model with cylindrical boundary conditions [24]. Under this approximation, the number density of antideuterons per unit energy, $f_{\bar{d}}(E, \vec{r}, t)$, satisfies the following transport equation:

$$0 = \frac{\partial f_{\bar{d}}}{\partial t} = \vec{\nabla} \cdot [K(E, \vec{r}) \vec{\nabla} f_{\bar{d}} - \vec{V}_c(\vec{r}) f_{\bar{d}}] + Q(E, \vec{r}) . \quad (9)$$

where we have neglected non-annihilating interactions of antideuterons with the interstellar gas, as well as the changes in the energy of the antideuteron during their propagation due to energy losses and reacceleration.² The boundary conditions require the solution $f_{\bar{d}}(E, \vec{r}, t)$ to vanish at the boundary of the diffusion zone, which is approximated by a cylinder with half-height $L = 1 - 15$ kpc and radius $R = 20$ kpc.

The first term on the right-hand side of the transport equation is the diffusion term, which accounts for the propagation through the tangled Galactic magnetic field. The diffusion coefficient $K(E, \vec{r})$ is assumed to be constant throughout the diffusion zone and is parametrized by:

$$K(E) = K_0 \beta \mathcal{R}^\delta , \quad (10)$$

²This assumption is well justified for antideuterons from dark matter decay, since after being produced in the Milky Way halo, they rarely cross the disk before reaching the Earth.

where $\beta = v/c$ and \mathcal{R} is the antideuteron rigidity, which is defined as the momentum in GeV per unit charge, $\mathcal{R} \equiv p(\text{GeV})/Z$. The normalization K_0 and the spectral index δ of the diffusion coefficient are related to the properties of the interstellar medium and can be determined from the flux measurements of other cosmic ray species, mainly from the Boron-to-Carbon (B/C) ratio [25].

The second term is the convection term, which accounts for the drift of charged particles away from the disk induced by the Milky Way's Galactic wind. It has axial direction and is also assumed to be constant inside the diffusion region: $\vec{V}_c(\vec{r}) = V_c \text{sign}(z) \vec{e}_z$. The third term accounts for antimatter annihilation when it interacts with ordinary matter in the Galactic disk, which is assumed to be an "infinitely" thin disk with half-width $h = 100$ pc. The annihilation rate, Γ_{ann} , is given by:

$$\Gamma_{\text{ann}} = (n_{\text{H}} + 4^{2/3} n_{\text{He}}) \sigma_{\bar{d}p}^{\text{ann}} v. \quad (11)$$

In this expression it has been assumed that the annihilation cross section between an antideuteron and a helium nucleus is related to the annihilation cross section between an antideuteron and a proton by the simple geometrical factor $4^{2/3}$. On the other hand, $n_{\text{H}} \sim 1 \text{ cm}^{-3}$ is the number density of Hydrogen nuclei in the Milky Way disk, $n_{\text{He}} \sim 0.07 n_{\text{H}}$ the number density of Helium nuclei and $\sigma_{\bar{d}p}^{\text{ann}}$ is the annihilation cross section. No experimental data are available for the $\bar{d}p$ collisions, although measurements exist for the total cross section of the charge-conjugated process $d\bar{p} \rightarrow X$. Since strong interactions preserve charge conjugation, it is reasonable to assume that $\sigma_{\bar{d}p}^{\text{tot}} = \sigma_{d\bar{p}}^{\text{tot}}$. However, it is not the total cross section that is required to compute the depletion of antideuterons during their propagation, but the annihilation cross section. Unfortunately, there is no experimental information about the annihilation cross section neither for $\bar{d}p$ nor for $d\bar{p}$ collisions. However, it was noted in [13] that the total cross section for $d\bar{p} \rightarrow X$ can be well approximated, within $\sim 10\%$, by $2\sigma_{p\bar{p}}^{\text{tot}}$ and hence $\sigma_{\bar{d}p}^{\text{tot}} \simeq 2\sigma_{p\bar{p}}^{\text{tot}}$. Then, assuming that the same rule applies for the annihilation cross section, one obtains $\sigma_{\bar{d}p}^{\text{ann}} \simeq 2\sigma_{p\bar{p}}^{\text{ann}}$. For our numerical analysis, we will adopt the parametrization by Tan and Ng of the proton-antiproton annihilation cross section [26]:

$$\sigma_{p\bar{p}}^{\text{ann}}(T_{\bar{p}}) = \begin{cases} 661 (1 + 0.0115 T_{\bar{p}}^{-0.774} - 0.948 T_{\bar{p}}^{0.0151}) \text{ mbarn}, & T_{\bar{p}} < 15.5 \text{ GeV}, \\ 36 T_{\bar{p}}^{-0.5} \text{ mbarn}, & T_{\bar{p}} \geq 15.5 \text{ GeV}, \end{cases} \quad (12)$$

where $T_{\bar{p}}$ is the kinetic energy of the antiproton.

Model	δ	K_0 (kpc ² /Myr)	L (kpc)	V_c (km/s)
MIN	0.85	0.0016	1	13.5
MED	0.70	0.0112	4	12
MAX	0.46	0.0765	15	5

Table 2: Astrophysical parameters compatible with the B/C ratio that yield the minimal (MIN), median (MED) and maximal (MAX) flux of antideuterons.

The solution of the transport equation at the Solar System, $r = r_\odot$, $z = 0$, can be formally expressed by the convolution

$$f_{\bar{d}}(E_{\bar{d}}) = \frac{1}{m_{\text{DM}}\tau_{\text{DM}}} \int_0^{m_{\text{DM}}} dE'_{\bar{d}} G_{\bar{d}}(E_{\bar{d}}, E'_{\bar{d}}) \frac{dN_{\bar{d}}(E'_{\bar{d}})}{dE'_{\bar{d}}}. \quad (13)$$

The analytic expression for the Green's function reads [27]:

$$G_{\bar{d}}(T, T') = \sum_{i=1}^{\infty} \exp\left(-\frac{V_c L}{2K(T)}\right) \frac{y_i(T)}{A_i(T) \sinh(S_i(T)L/2)} J_0\left(\zeta_i \frac{r_\odot}{R}\right) \delta(T - T'), \quad (14)$$

where

$$y_i(T) = \frac{4}{J_1^2(\zeta_i) R^2} \int_0^R r' dr' J_0\left(\zeta_i \frac{r'}{R}\right) \int_0^L dz' \exp\left(\frac{V_c(L-z')}{2K(T)}\right) \sinh\left(\frac{S_i(L-z')}{2}\right) \rho(\vec{r}'), \quad (15)$$

and

$$A_i(T) = 2h\Gamma_{\text{ann}}(T) + V_c + kS_i(T) \coth\frac{S_i(T)L}{2}, \quad (16)$$

$$S_i(T) = \sqrt{\frac{V_c^2}{K(T)^2} + \frac{4\zeta_i^2}{R^2}}. \quad (17)$$

We find that the Green's function can be numerically approximated by the following interpolation function:

$$G_{\bar{d}}(T, T') \simeq 10^{14} e^{x+y \ln T + z \ln^2 T} \delta(T' - T) \text{ cm}^{-3} \text{ s}, \quad (18)$$

which is valid for any decaying dark matter particle. The coefficients x , y and z for the NFW profile can be found in Table 3 for the various diffusion models in Table 2; the dependence of the Green's function on the halo model is fairly weak. In this case the approximation is better than about 5% for $T_{\bar{d}}$ between 1 and 100 GeV/n and better than about 20% for $T_{\bar{d}}$ between 0.1 and 1 GeV/n.

model	x	y	z
MIN	-0.3889	0.7532	-0.1788
MED	1.6023	0.4382	-0.1270
MAX	3.1992	-0.1098	-0.0374

Table 3: Coefficients of the interpolating function Eq. (18) for the antideuteron Green’s function for the NFW halo profile.

Finally, the flux of primary antideuterons at the Solar System from dark matter decay is given by:

$$\Phi_{\bar{d}}^{\text{prim}}(E_{\bar{d}}) = \frac{v}{4\pi} f_{\bar{d}}(E_{\bar{d}}), \quad (19)$$

where v is the velocity of the antideuteron.

However, this is not the antideuteron flux measured by balloon or satellite experiments, which is affected by solar modulation. In the force field approximation [28] the effect of solar modulation can be included by applying the following simple formula that relates the antideuteron flux at the top of the Earth’s atmosphere and the interstellar antideuteron flux [29]:

$$\Phi_{\bar{d}}^{\text{TOA}}(T_{\text{TOA}}) = \left(\frac{2m_{\bar{d}}T_{\text{TOA}} + T_{\text{TOA}}^2}{2m_{\bar{d}}T_{\text{IS}} + T_{\text{IS}}^2} \right) \Phi_{\bar{d}}^{\text{IS}}(T_{\text{IS}}), \quad (20)$$

where $T_{\text{IS}} = T_{\text{TOA}} + \phi_F$, with T_{IS} and T_{TOA} being the antideuteron kinetic energies at the heliospheric boundary and at the top of the Earth’s atmosphere, respectively, and ϕ_F being the solar modulation parameter, which varies between 500 MV and 1.3 GV over the eleven-year solar cycle. Since experiments are usually undertaken near solar minimum activity, we will choose $\phi_F = 500$ MV for our numerical analysis in order to compare our predicted flux with the collected data.

4 Antideuteron Flux at Earth from Dark Matter Decay

Using the injection spectrum of antideuterons from dark matter decay calculated in Section 2 and the propagation formalism described in Section 3, it is straightforward to calculate the antideuteron flux at Earth from dark matter decay.³ We will pursue here

³For calculations of the antideuteron flux from the annihilation of dark matter particles, see [12,13,30].

a model-independent approach, calculating the expected antideuteron flux at Earth for various hadronic decay channels and different dark matter masses. To better compare the predictions for the different possibilities, we will first fix the dark matter lifetime to be $\tau_{\text{DM}} = 10^{26}\text{s}$, which is the order of magnitude which could explain the HEAT and PAMELA anomalies in the positron fraction [31,32,3,33] and which saturates the EGRET constraints on the diffuse gamma-ray flux [34,32]. Later on, we will discuss in more detail the predictions for the antideuteron flux in the light of the PAMELA anomaly.

In the case that the dark matter particle is a fermion ψ , the following hadronic decay channels are possible:

$$\begin{aligned}
\psi &\rightarrow Z^0\nu, \\
\psi &\rightarrow W^\pm\ell^\mp, \\
\psi &\rightarrow h^0\nu.
\end{aligned}
\tag{21}$$

The fragmentation of the weak gauge bosons and the Standard Model Higgs boson produces a flux of antideuterons which has been calculated using the coalescence model to simulate the nuclear fusion of an antiproton and an antineutron (*cf.* Section 2), and the event generator PYTHIA 6.4 [35], to simulate the production of individual antiprotons and antineutrons.

Clearly, an exotic contribution to the antideuteron flux is correlated with an exotic contribution to the antiproton flux, which is severely constrained by a number of experiments. Namely, the measurements of the antiproton flux by PAMELA [5], BESS95 [6], BESS95/97 [7], CAPRICE94 [8], CAPRICE98 [9] and IMAX [10] do not show any significant deviation from the predictions by conventional astrophysical models of spallation of cosmic rays on the Milky Way disk. Therefore, in order to evaluate the prospects of observing the antideuteron flux in future experiments, one has to ensure that the prediction for the total antiproton flux does not exceed the observed flux. The antiproton flux from dark matter decay has been calculated following the analysis in [31], for the same propagation models as for the antideuteron flux.

We show in Figs. 1, 2, 3 the antiproton and antideuteron fluxes from dark matter decay as a function of the kinetic energy per nucleon, assuming that the dark matter particle is a fermion ψ , which decays exclusively into $Z^0\nu$, $W^\pm\ell^\mp$ or $h^0\nu$, respectively. The lifetime has been fixed to $\tau_{\text{DM}} = 10^{26}\text{s}$, while the dark matter mass has been

chosen to be $m_{\text{DM}} = 200, 400, 600, 800$ GeV. The predictions for the antiproton and antideuteron fluxes for a general model with a different dark matter lifetime and with arbitrary branching ratios can be straightforwardly derived from these figures. In each plot, we show the prediction for the antiproton and antideuteron fluxes at the top of the atmosphere for the MIN, MED and MAX propagation models (see table 2) as well as the expected flux from spallation, taken from [27] in the case of the antiprotons and from [13] in the case of the antideuterons.⁴ For the halo model, we adopted the Navarro-Frenk-White (NFW) profile; the results for other halo profiles are very similar to the ones presented here. We also show the present upper limit on the antideuteron flux from BESS [14], as well as the projected limits for AMS-02 for three years of data taking [15,16], as well as for GAPS [17,18] for a long duration balloon (LDB) flight (60 days total over three flights) and for an ultra-long duration balloon (ULDB) flight (300 days total).

For this particular choice of the lifetime, $\tau_{\text{DM}} = 10^{26}$ s, we find wide ranges of diffusion parameters yielding a total antiproton flux consistent with the observations. Besides, the total antideuteron flux always lies well below the present BESS bound. We also find that for dark matter masses below ~ 1 TeV, the antideuteron flux from dark matter decay can be, at energies below 3 GeV, significantly larger than the secondary antideuteron flux from spallation. Furthermore, the primary antideuteron flux from dark matter decay could be large enough to be observable at the projected experiments AMS-02 and GAPS. Therefore, since the purely secondary antideuteron flux is expected to be below the sensitivity of projected experiments, the observation of an antideuteron flux in the near future could be interpreted as a signature of dark matter particles which decay hadronically.

When the decaying dark matter particle is a scalar, the following hadronic decay modes are possible:

$$\begin{aligned}
\phi &\rightarrow Z^0 Z^0, \\
\phi &\rightarrow W^+ W^-, \\
\phi &\rightarrow h^0 h^0.
\end{aligned}
\tag{22}$$

⁴In these plots we only show the prediction for the secondary antiproton and antideuteron fluxes for the MED propagation model. Whereas the uncertainty on the propagation model is typically not very important for the prediction of the secondary fluxes, there exists a more important source of uncertainty stemming from the nuclear and hadronic cross sections, which can be as large as 25% for antiprotons [27] and 100% for antideuterons [13].

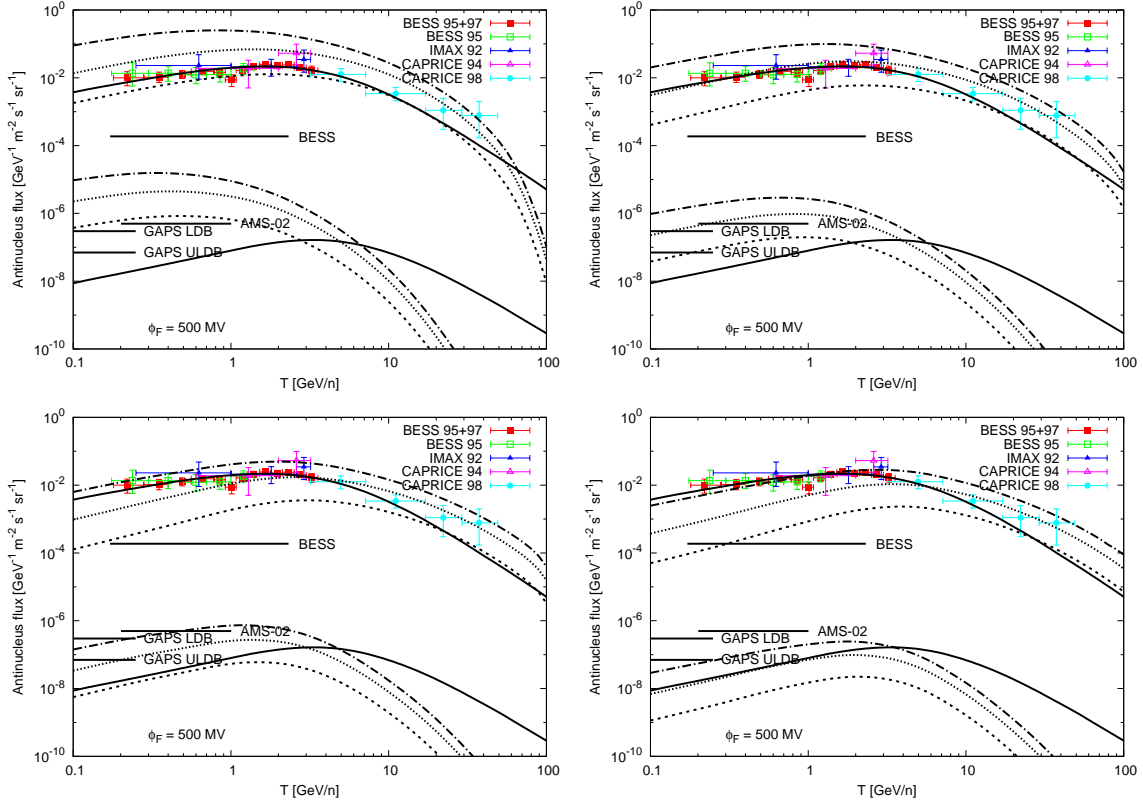


Figure 1: Fluxes of antiprotons (upper curves) and antideuterons (lower curves) from the decay of fermionic dark matter particles, assuming that the dark matter particle decays exclusively as $\psi \rightarrow Z^0\nu$ with a fixed lifetime $\tau_{\text{DM}} = 10^{26}\text{s}$. The dark matter mass is 200 GeV (top left panel), 400 GeV (top right), 600 GeV (bottom left) and 800 GeV (bottom right). The dashed lines indicate the primary fluxes from dark matter decay for the MIN propagation model, the dotted lines for the MED propagation model, and the dash-dotted lines for the MAX propagation model (*cf.* Table 2). The solid lines indicate the secondary fluxes.

In these cases, the produced antideuteron flux is approximately twice as large as in the fermionic channels, $\psi \rightarrow Z^0\nu$, $\psi \rightarrow W^\pm\ell^\mp$, $\psi \rightarrow h^0\nu$, respectively, and will not be discussed further.

Let us now discuss the prospects for the detection of an antideuteron flux in projected experiments, assuming that dark matter decay is the explanation of the positron excess reported by the PAMELA and HEAT collaborations. As discussed in [3], the steep rise of the positron fraction measured by PAMELA can be explained by the decay of a dark matter particle into hard electrons and positrons. Namely, in the case that the dark matter particle is a fermion, the decay modes $\psi \rightarrow e^+e^-\nu$ and $\psi \rightarrow W^\pm e^\mp$ (and

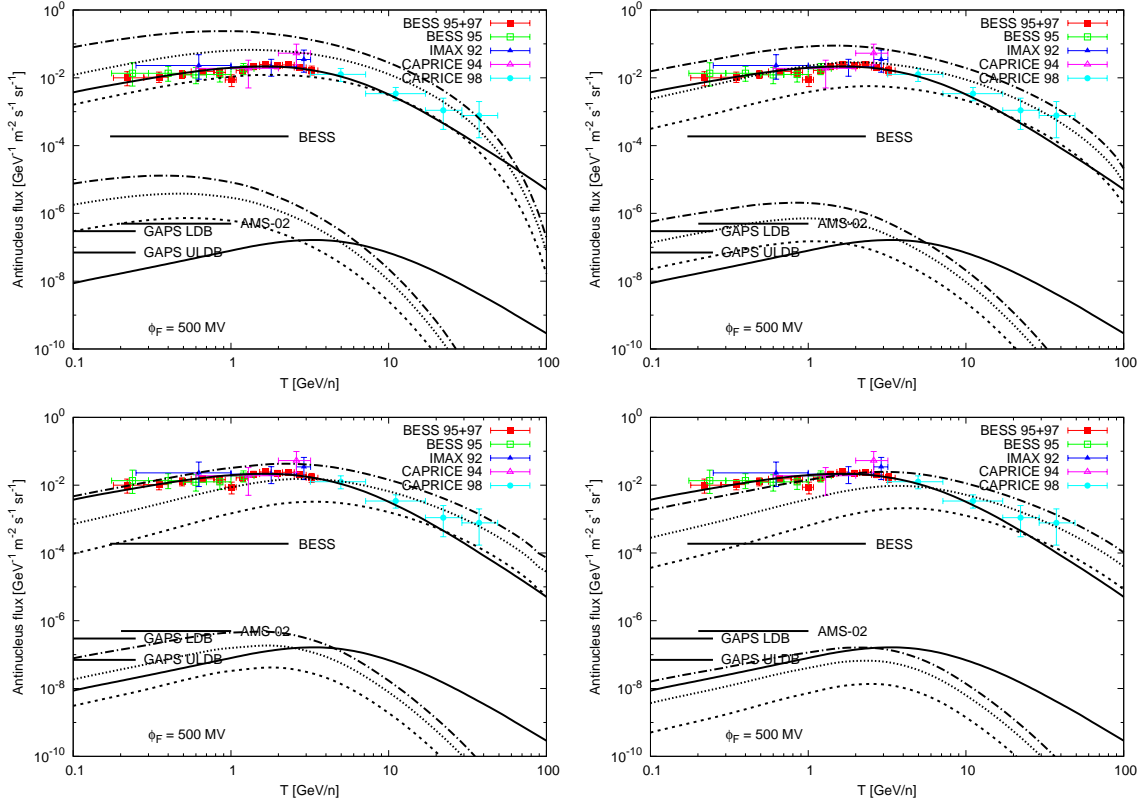


Figure 2: The same as Fig. 1 for the decay mode $\psi \rightarrow W^\pm \ell^\mp$.

the analogous decay modes into muon flavor) are favored by the data. On the other hand, when the dark matter particle is a scalar, the decay modes $\phi \rightarrow e^+e^-$, $\mu^+\mu^-$ are favored. Purely leptonic decay modes, such as $\psi \rightarrow \ell^+\ell^-\nu$ or $\phi \rightarrow \ell^+\ell^-$ do not produce antideuterons. However, as discussed above, the decay of a fermionic dark matter particle into W^\pm bosons and charged leptons could produce an observable antideuteron flux.

We show in Fig. 4 the total antiproton and antideuteron fluxes from the decay of a fermionic dark matter particle in the channel $\psi \rightarrow W^\pm e^\mp$, fixing for each dark matter mass the lifetime in order to account for the step rise in the positron fraction observed by PAMELA. For a dark matter mass $m_{\text{DM}} = 300, 600, 1000$ GeV, the corresponding lifetimes are $\tau_{\text{DM}} = 4.0, 2.3, 1.6 \times 10^{26}$ s, respectively. For these particularly interesting decaying dark matter scenarios, we find that the antideuteron flux could be within the reach of the planned experiments AMS-02 and GAPS, provided the dark matter particle is not too heavy. The discovery of antideuterons would thus favor the decay

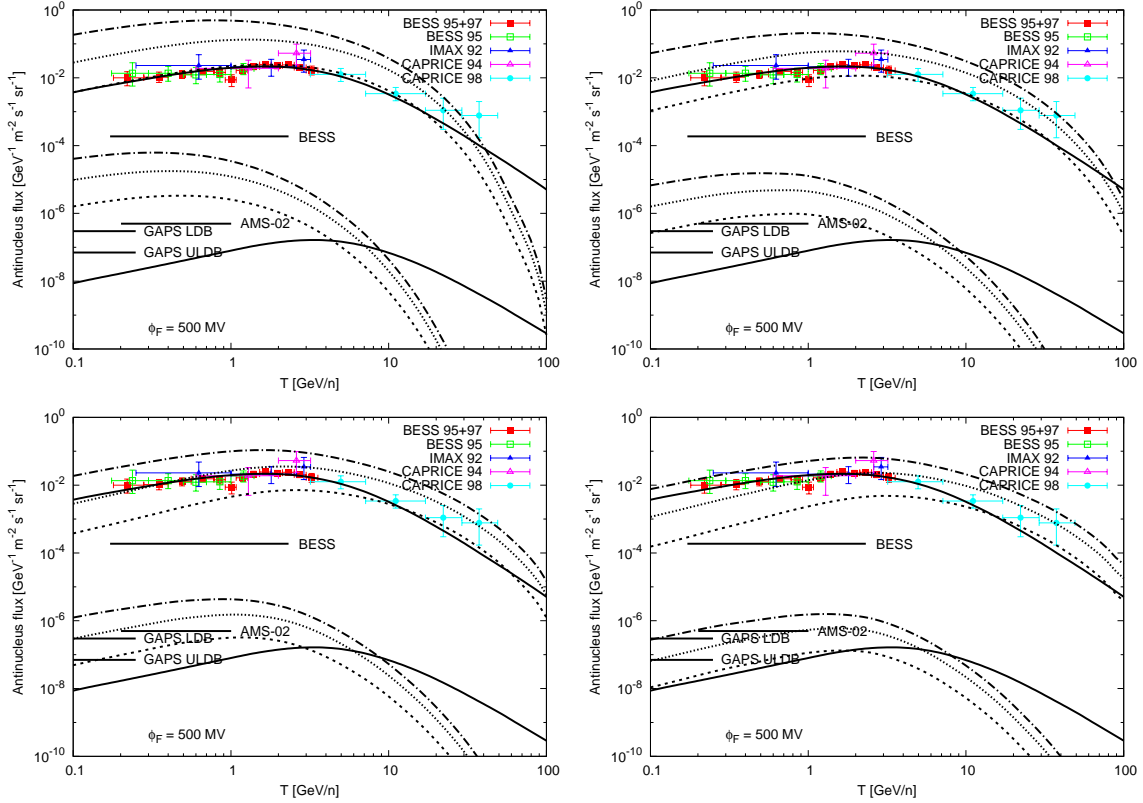


Figure 3: The same as Fig. 1 for the decay mode $\psi \rightarrow h^0\nu$.

mode $\psi \rightarrow W^\pm e^\mp$ as a possible origin of the PAMELA positron excess over the purely leptonic decay modes such as $\psi \rightarrow e^+e^-\nu$.⁵ It is important to emphasize that this conclusion holds for ranges of propagation parameters which not only reproduce the positron excess observed by PAMELA, but also yield a total antiproton flux consistent with present measurements.

5 Conclusions

We have calculated the antideuteron fluxes at Earth from the decay of dark matter particles in the Milky Way halo and we have discussed the prospects to observe cosmic antideuterons in the projected experiments AMS-02 and GAPS. We have adopted a model-independent approach analyzing possible hadronic decay modes for the dark matter particle. The nuclear fusion of an antiproton and an antineutron to form an-

⁵The decay mode $\psi \rightarrow W^\pm e^\mp$ may also yield signatures in the diffuse gamma-ray background.

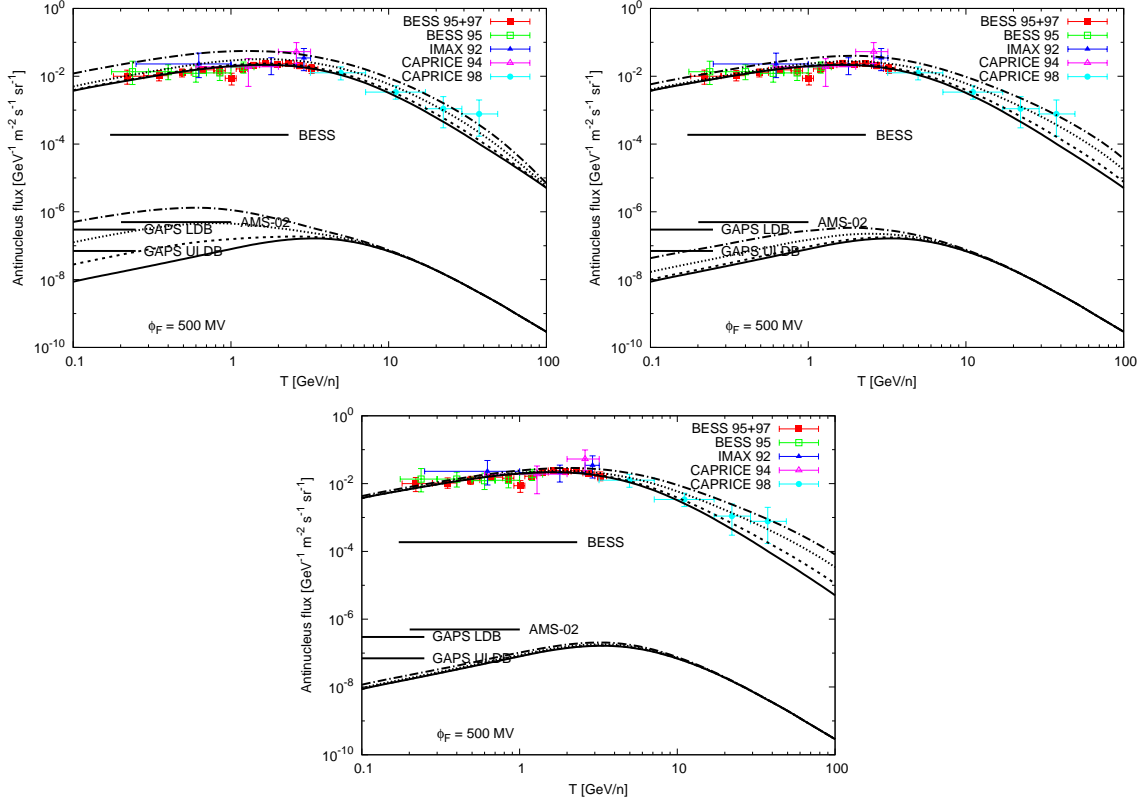


Figure 4: Total antiproton and antideuteron fluxes including a primary contribution to the flux from the decay of a fermionic dark matter particle in the channel $\psi \rightarrow W^\pm e^\mp$. The lifetime has been chosen, for each dark matter mass, to reproduce the steep rise in the positron fraction observed by the PAMELA collaboration. When the dark matter mass is 300 GeV (top left panel), 600 GeV (top right panel) and 1000 GeV (bottom panel), the corresponding lifetimes are $\tau_{\text{DM}} = 4.0, 2.3, 1.6 \times 10^{26}$, respectively. The dashed lines indicate the total fluxes for the MIN propagation model, the dotted lines for the MED propagation model, and the dash-dotted lines for the MAX propagation model (*cf.* Table 2). We also show the purely secondary fluxes as solid lines.

tideuteron was simulated employing the coalescence model, while the propagation of antideuterons in the Galaxy was described by a stationary two-zone diffusion model with cylindrical boundary conditions. The hadronic showers also produce a flux of primary antiprotons, which is severely constrained by observations. Therefore, we have simultaneously calculated the predicted antiproton flux, to verify whether the chosen parameters and decay modes are consistent with present observations.

We have shown that there are choices of parameters where the antideuteron flux from dark matter decay can be much larger than the purely secondary component from spallation of cosmic rays on the interstellar medium, while at the same time the total antiproton flux remains consistent with observations. We have also shown that if the dark matter particle is sufficiently light, the antideuteron flux from dark matter decay could be within the reach of the planned experiments AMS-02 or GAPS, while the secondary component is expected to lie below the sensitivity of planned experiments. Therefore, the observation of cosmic antideuterons in the near future could be interpreted as an indication for hadronic decays of dark matter particles. In particular, this conclusion holds for a fermionic dark matter particle which decays preferentially via $\psi \rightarrow W^\pm e^\mp$, which has been proposed as an explanation for the steep rise in the positron fraction observed by the PAMELA collaboration.

Acknowledgements

This work was partially supported by the DFG cluster of excellence “Origin and Structure of the Universe.”

References

- [1] G. Bertone, D. Hooper and J. Silk, Phys. Rept. **405** (2005) 279.
- [2] O. Adriani *et al.* [PAMELA Collaboration], arXiv:0810.4995 [astro-ph].
- [3] A. Ibarra and D. Tran, JCAP **0902** (2009) 021.
- [4] P. Sreekumar *et al.* [EGRET Collaboration], Astrophys. J. **494** (1998) 523.
- [5] O. Adriani *et al.*, Phys. Rev. Lett. **102** (2009) 051101.

- [6] H. Matsunaga *et al.*, Phys. Rev. Lett. **81** (1998) 4052.
- [7] S. Orito *et al.* [BESS Collaboration], Phys. Rev. Lett. **84** (2000) 1078.
- [8] M. Boezio *et al.* [WIZARD Collaboration], Astrophys. J. **487** (1997) 415.
- [9] M. Boezio *et al.* [WiZard/CAPRICE Collaboration], Astrophys. J. **561** (2001) 787.
- [10] J. W. Mitchell *et al.*, Phys. Rev. Lett. **76** (1996) 3057.
- [11] A. W. Strong, I. V. Moskalenko and O. Reimer, Astrophys. J. **613** (2004) 962.
- [12] F. Donato, N. Fornengo and P. Salati, Phys. Rev. D **62** (2000) 043003;
- [13] F. Donato, N. Fornengo and D. Maurin, Phys. Rev. D **78** (2008) 043506.
- [14] H. Fuke *et al.*, Phys. Rev. Lett. **95** (2005) 081101.
- [15] V. Choutko and F. Giovacchini, on behalf of the AMS Collaboration, Proceeding of the 30th International Cosmic Ray Conference (2007).
- [16] J. E. Koglin *et al.*, J. Phys. Conf. Ser. **120** (2008) 042011.
- [17] C. J. Hailey *et al.*, Nucl. Instrum. Meth. B **214** (2004) 122.
- [18] C. J. Hailey *et al.*, JCAP **0601** (2006) 007.
- [19] L. Bergstrom, P. Ullio and J. H. Buckley, Astropart. Phys. **9** (1998) 137.
- [20] J. F. Navarro, C. S. Frenk and S. D. M. White, Astrophys. J. **462** (1996) 563.
- [21] B. Moore, T. Quinn, F. Governato, J. Stadel and G. Lake, Mon. Not. Roy. Astron. Soc. **310** (1999) 1147.
- [22] R. Duperray *et al.*, Phys. Rev. D **71** (2005) 083013.
- [23] S. Schael *et al.* [ALEPH Collaboration], Phys. Lett. B **639** (2006) 192.
- [24] See for example V. S. Berezinskii, S. V. Buolanov, V. A. Dogiel, V. L. Ginzburg, V. S. Ptuskin, Astrophysics of Cosmic Rays (Amsterdam: North-Holland, 1990).
- [25] D. Maurin, F. Donato, R. Taillet and P. Salati, Astrophys. J. **555** (2001) 585.

- [26] L. C. Tan and L. K. Ng, *J. Phys. G* **9** (1983) 227.
- [27] F. Donato, D. Maurin, P. Salati, R. Taillet, A. Barrau and G. Boudoul, *Astrophys. J.* **563** (2001) 172.
- [28] L. J. Gleeson and W. I. Axford, *Astrophys. J.* **149** (1967) L115; *Astrophys. J.* **154** (1968) 1011.
- [29] J. S. Perko, *Astron. Astrophys.* **184** (1987) 119.
- [30] C. B. Bräuninger and M. Cirelli, arXiv:0904.1165 [hep-ph].
- [31] A. Ibarra and D. Tran, *JCAP* **0807** (2008) 002.
- [32] K. Ishiwata, S. Matsumoto and T. Moroi, *Phys. Rev. D* **78** (2008) 063505.
- [33] P. f. Yin, Q. Yuan, J. Liu, J. Zhang, X. j. Bi and S. h. Zhu, *Phys. Rev. D* **79** (2009) 023512; K. Ishiwata, S. Matsumoto and T. Moroi, arXiv:0811.0250 [hep-ph]; C. R. Chen, F. Takahashi and T. T. Yanagida, *Phys. Lett. B* **671** (2009) 71, *Phys. Lett. B* **673** (2009) 255.
- [34] W. Buchmuller, L. Covi, K. Hamaguchi, A. Ibarra and T. Yanagida, *JHEP* **0703** (2007) 037; G. Bertone, W. Buchmuller, L. Covi and A. Ibarra, *JCAP* **0711** (2007) 003; A. Ibarra and D. Tran, *Phys. Rev. Lett.* **100** (2008) 061301.
- [35] T. Sjostrand, S. Mrenna and P. Skands, *JHEP* **0605** (2006) 026.